We were not able to investigate the *in vivo* distribution of the injected tracer due to technical limitation, but we consider that the nanoparticle may distribute to reticuloendothelial system as described in previous reports [7-9], or may be excreted from kidney for their hydrophilia.

We histologically observed liver and kidney two weeks after subcutaneous injection of fluorescent beads. Consequently, we didn't find beads trapped in liver or kidney by fluorescent microscopic observation, suggesting that the safety of these beads would be ensured when they are given *in vivo*.

Additionally, the fluorescent beads that we used at this time for these experiments are mainly consisted of polystyrene. As polystyrene is the material often used for surgical strings in operation, there would be safe when we gave fluorescent beads to living organisms. Accumulation and long term toxicity are under investigation.

The sample depth is a very serious problem in fluorescence measurement of living tissue. The local excitation illumination within tissue exponentially attenuates due to absorption and scattering from the surface to that depth. This problem of lack of transmission prevents us from detection in tissues deeper than 1 cm from the surface of the body at present [10]. We can detect the SN of small animals like rats, but may have difficulty in detection in larger animals because of the depth at which SNs exist (*i.e.*, more than 1cm away from the skin surface). For example, lymph node in human is buried in fat and it locates deeper than 1 cm. Detection technique to find SN up to 2 cm depth is recommended. Therefore, we are investigating the application of semiconductor nano crystal that has extremely stronger fluorescent intensity than usual fluorescent beads to increase the detection ability, with an improvement of technique including time/frequency domain spectrometry.

We confirmed that fluorescent beads have the potential to be an alternative to existing tracers in the detection of the SN in animal experiments if we select the appropriate particle size and wavelength.

We experimented to identify SN by traditional dye method using patent blue for comparison of fluorescent beads. We tested 20 hind legs of 10 rats. Patent blue was subcutaneously injected at the foot pad of the hind leg as well as fluorescent beads and checked whether inguinal nodes were visible. We identified inguinal nodes in 8 of 20 legs by dye, whereas, we identified 24 of 31 legs by fluorescent beads at DR 40nm. Detection rate was significantly higher with using fluorescent beads as tracer (data not shown). We are now preparing for an experiment to clarify the superiority of fluorescent method with conventional dye method for clinical application.

Acknowledgments

This work was supported by Grants-in-aid for Research Project, Promotion of Advanced Medical Technology (H14-Nano-010), from the Ministry of Health, Labor and Welfare of Japan. We also acknowledge the support of Tohoku University 21st Century Center of Excellence (COE) Program "Future Medical Engineering based on Bio-nanotechnology".

References

[1] Morton DL, Wen DR, Wong JH, Economou JS, Cagle LA, Storm FK, Foshag LJ, and Cochran AJ. Technical details of intraoperative lymphatic mapping for early stage melanoma. *Arch Surg* **127**, 392-399, 1992.
[2] Giuliano AE, Kirgan DM, Guenther JM, and Morton DL. Lymphatic mapping and sentinel lymphadenectomy for breast cancer. *Ann Surg* **220**, 391-401, 1994.
[3] Krag DN, Weaver DL, Alex JC, and Fairbank JT. Surgical resection and radio-localization of the sentinel node in breast cancer using a gamma probe. *Surg Oncol* **2**, 335-340, 1993.
[4] Tafra L, Lannin DR, Swanson MS, Van Eyk JJ, Verbanac KM, Chua AN, Ng PC, Edwards MS, Halliday BE, Henry CA, Sommers LM, Carman CM, Molin MR, Yurko JE, Perry RR, and Williams R. Multicenter trial of sentinel node biopsy for breast cancer using both technetium sulfur colloid and isosulfan blue dye. *Ann Surg* **233**, 51-59, 2001.
[5] Moghimi SM and Bonnemain B. Subcutaneous and intravenous delivery of diagnostic agents to the lymphatic system: applications in lymphoscintigraphy and indirect lyphography. *Advanced Drug Delivery Reviews* **37**, 295-312, 1999.
[6] Ikomi F, Hanna G, and Schmid-Schonbein GW. Mechanism of colloidal particle uptake into the lymphatic system. *Radiology* **196**, 107-113, 1995.
[7] Josephson L, Mahmood U, Wunderbaldinger P, Tang Y, and Weissleder R. Pan and sentinel lymph node visualization using a near-infrared fluorescent probe. *Mol Imaging* **2**, 18-23, 2003.
[8] Patrick W, Karl T, and Chrstoph B. Near-Infrared fluorescence imaging of lymph nodes using a new enzyme sensing activatable macromolecular optical probe. *Eur Radiol* **13**, 2206-2211, 2003.
[9] Ann EH, Lisbeth I, and Stanley SD. Lymph node localization of biodegradable nanospheres surface modified with poloxamer and poloxamine block co-polymer. *FEBS Letters* **400**, 319-323, 1997.
[10] Yang M, Baranov E, Jiang P, Sun FX, Li XM, Li L, Hasegawa S, Bouvet M, AI-Tuwaijri M, Chishima T, Shimada H, Moossa AR, Penman S, and Hoffman RM. Whole-body optical imaging of green fluorescent protein-expressing tumors and metastasis. *Proc Natl Acad Sci USA* **97**, 1206-1211, 1997.

IN VIVO BREAST CANCER CELL IMAGING USING QUANTUM DOT CONJUGATED WITH ANTI-HER2 ANTIBODY

HIROSHI TADA [1)†], HIDEO HIGUCHI [2)], TOMONOBU M. WATANABE [2)], NORIAKI OHUCHI[1)]

1) Department of Surgical Oncology, Graduate School of Medicine, Tohoku University, Sendai, Japan

2) Biomedical Engineering Research Organization, Tohoku University, Sendai, Japan

Semiconductor quantum dots (Qdot) are nanometer-sized crystals which improved brightness, resistance against photobleaching compared with organic dyes and fluorescent proteins. Therefore, Qdot are thought to become new adjuncts of fluorescent bioprobes for medical applications, especially for cancer imaging. We have used Qdot conjugated with monoclonal anti-HER2 antibody (Trastuzumab) for molecular imaging of breast cancer cells. We utilized poly ethylene glycol (PEG) coated Qdot-Trastuzumab complex to label a cell membrane of HER2 overexpressing breast cancer cells. Using this complex, we established the *in vivo* fluorescent cancer imaging method. After injection of the Qdot-Trastuzumab complex to the human breast cancer xenograft mouse model, the accumulation of Qdot to the tumor tissue was clearly observed at subcellular resolution with the original 3D intravital microscopic system. This suggests that we can eventually develop a novel cancer imaging and drug tracking system.

Keywords: Breast cancer, HER2, Molecular imaging, Quantum dots.

1. Introduction

Recent advances in nanotechnology have produced new fluorescent semiconductor nanocrystals (quantum dots: Qdot). Compared with classical organic fluorescent dyes, Qdot have unique luminescent properties; fluorescence emission is very intensive and stable for a long time [1-3]. Therefore Qdots are thought to have a potential as novel probes for clinical diagnosis for cancer imaging and many other issues under in vivo circumstance.

We have explored the *in vivo* 3D cancer imaging using Qdot conjugated with trastuzumab. Trastuzumab is a monoclonal anti-HER2 antibody as anticancer drug, which accumulation and retention of at the site of tumor is the

†Hiroshi Tada was a Tohoku University 21COE Research Assistant from 2002 to 2004.

basis of radioimmunoscintigraphic scanning and targeted therapy for human HER2 overexpressing breast cancer metastasis [4-6].

In order to observe Qdot in tumor tissue, we constructed the high resolutional intravital imaging system. This system consists of the confocal scanner unit employing a Nipkow type disc and the electron miultiplying charge coupled device (EMCCD) camera. The confocal unit adopts multi-beam scanning using about a thousand beams that are simultaneously emitted through a pin-hole disk to facilitate high-speed scanning. And the EMCCD has advantage that offering unsurpassed sensitivity performance, and has been shown to yield markedly improved S/N (signal / noise) ratio. This system facilitates the high resolution *in vivo* 3D imaging.

Here, we report the development of the *in vivo* fluorescence 3D imaging of breast cancer cells in living mouse breast cancer xenograft model using Qdot-Trastuzumab complex.

2. Materials and Methods

Semiconductor quantum dots: Qdot are made from semiconductor material (core: CdTe) which has been coated with an additional semiconductor shell (ZnS). This core-shell material is further coated with polyethylene glycol (PEG), which greatly reduces non-specific binding and immune response.

Preparation of Qdot conjugates: Qdot was conjugated to trastuzumab (Herceptin, Chugai pharmaceutical co., LTD., Tokyo, Japan.) with a Qdot 800 Antibody Conjugation Kit (Quantum dot corporation, Hayward, CA) via poly ethylene glycol (Mw. 2000), and SMCC-croslinkers. The final concentration of QT-complexes was determined by measuring the conjugate absorbance at 550 nm and using an extinction coefficient of 1,700,000 $M^{-1}cm^{-1}$ at 550 nm.

Cell line and human cancer xenograft model: The human breast cancer cell line, KPL-4 which overexpresses HER2 and is sensitive to trastuzumab was kindly provided by Dr. J. Kurebayashi (Kawasaki Medical school, Kurashiki, Japan) [7, 8]. KPL-4 cells were cultured in Dulbecco's modified Eagle's medium (DMEM) supplemented with 5% fetal bovine serum. A suspension of KPL-4 ($0.8x10^7$ cells/mouse) was orthotopically transplanted subcutaneously to the dorsal skin of the female BALB/c nu/nu mice at 6-10 weeks of age (Charles River Japan, Yokohama, Japan). Several weeks after tumor inoculation, mice bearing a tumor volume of 100-200mm^3 were selected. All of the mice were maintained in our pathogen-free institutional facilities. All operations on animals were in according with institutional animal use and care regulations.

Imaging system: The optics system for 3D observation was consisted primarily of an epi-fluorescent microscope (IX71, Olympus), a nipkow lens type confocal unit (CSU10, Yokokawa) and an electron multiplier type CCD camera (iXon 887, Andor). The object lens (x60, N.A. 1.45) was moved by a piezo actuator with a feedback loop (Nanocontrol). A computer controlled the piezo actuator in synchronization with the image acquisitions in order that the object lens remained within the exposure time of the CCD camera. An area ~30x30μm^2 was illuminated by a green laser (532 nm, Crystalaser).

In vivo imaging: QT-complexes were injected into the tail vein of mice at a concentration 0.2 nmol. The mice were placed under anesthesia by injection of ketamine and xylazine mixture intraperitoneally at dosages of 95mg/kg and 5 mg/kg, respectively. The temperature of mice was maintained at 37 °C by thermo-plate and objective lens heater.

The dorsal skin fold chamber, described previously (REF) and modified for this study, was used to fix the exposed tumor of mice on the microscopic stage. Two sterilized polyvinyl chloride plates (0.5mm thickness) containing a window were mounted so as to fix the extended double layer of dorsal skin including a tumor site. Skin plus the chambers were sutured by 6-0 nylon around the window because tumor must be located in the center of the window and be fixed without be affected by the beating of the heart and breathing movements. The tumor was exposed by oval incision ~10 mm in diameter, and the subcutaneous connective tissue was removed. The tumor was then placed surface down on the neutral saline mounted cover slip on a viewing platform of an inverted microscope. The mouse was fixed to a metal plate on the stage designed to stabilize the chamber. Tumors can be visualized directly using this preparation.

After imaging, the mice were killed by overdose CO_2. Tumor was removed and divided for histological Qdot uptake study and immunohistochemical analysis. For the histological Qdot uptake study, tumors were frozen and cryosectioned (6 μm thick), fixed with acetone at 0 °C and examined with an imaging system. For immunohistological examination, tumors were fixed in 10% neutral-buffered formalin overnight and then transferred into 70% ethanol before processing and paraffin embedding. Immunohistochemical analysis was performed on 6 μm thick paraffin sections using the Herceptest kit (Daco Corp, Carpenteria, CA).

3. Results

Qdot were conjugated to trastuzumab using a Qdot antibody conjugation kit (QT-complex). The molar ratio of trastuzumab to the Qdot was approximately

3:1. Cultured cells, KPL-4, in *in vitro* were mixed with QT-complexes which bound strongly to the KPL-4 cell membranes. Qdots without trastuzumab did not bind or accumulation in the KPL-4 cells. Another control study using AH109A cells, a HER2 negative cell line, also showed no binding of the QT-complexes.

3D intravital images of QT-complexes in xenograft model mice were taken by moving an objective. The tumor region was fixed on a microscope stage. Intravital microscopic observations of the tumor regions was performed without confounding influences of respiratory and pulsating body movement of mice. Three-dimensional images of the tumor could be taken by reconstructing multi-confocal images from the surface of the mice to a depth of 150 μm inside a tumor through the dorsal skin fold chamber. Fluorescence micro-angiography was performed after injection of the QT-complexes into a tail vein. The membranes of the KPL-4 tumor cells were clearly stained with QT-complexes at 6 hours after the injection. At 24 hours after injection, the QT-complexes had been internalized into the tumor cells. After imaging the tumor in the living mice, histological examination of chemically fixed tumors was performed to confirm that the fluorescence images of QT-complexes in the living mice is on the KPL-4 cells. QT-complexes under an epi-fluorescence microscope were located at cell membrane and near the nuclear membrane. An adjacent slice of the observed area was further stained immuno-histologically with the antibody, A0485, against HER2. The cell membrane in the adjacent slice was stained locally. confirming that the fluorescence images of QT-complexes were present at the membrane of tumor cells (data not shown). Unfortunately nonspecific liver and spleen uptake was still apparent, with little or no QD accumulation in the brain, the heart, the kidney or the lung. We did not observe any acute toxicity, even after 24h of circulation, caused by the intravenous administration of QT-complex (*i.e.*, overt thrombosis or signs of complement activation).

4. Discussion

We showed the development of bioconjugated QD probes suitable for *in vivo* targeting and imaging of human breast cancer cells growing in mice. Tumor targeting by QT-complex is an exciting prospect, as tumor sites and margin could be readily imaged at subcellular level. 3D intravital microscopy combined with Qdot and dorsal skin fold chamber preparations have provided powerful insight into gene expression, physiological function and drug delivery in tumor.

Quantum dots contain cadmium, which is toxic and might cause damage if the dots remain in the body. Though more studies are needed to determine

toxicity, many experimental reports indicate that quantum dots are safe in the short term [9-11]. We expected that 3D intravital imaging with Qdot described here, provides a powerful tool clarifying molecular mechanisms of cancer and modes of action of anti-cancer therapeutics.

5. Conclusion

The cancer cells expressing HER2 were visualized by the QT-complex in living mice at subcellular resolution, suggesting that we can eventually develop a novel cancer imaging system to target the primary and metastatic tumors. Nanocrystal semiconductor quantum dots conjugated with antibody may serve fundamentally as new materials controllable for medical purposes including cancer molecular imaging.

Acknowledgments

We are grateful to the support by Grants-in-aid for Research Project, Promotion of Advanced Medical Technology (H14-Nano-010 and H18-Nano-001), from the Ministry of Health, Labor and Welfare of Japan, and the support by Tohoku University 21st Century Center of Excellence (COE) Program "Future Medical Engineering based on Bio-nanotechnology".

References

[1] Wu X, Liu H, Liu J, Haley KN, Treadway JA, Larson JP, *et al.* Immunofluorescent labeling of cancer marker Her2 and other cellular targets with semiconductor quantum dots. *Nat Biotechnol* **21**, 41-46, 2003.

[2] Bruchez M Jr, Moronne M, Gin P, Weiss S, and Alivisatos AP. Semiconductor nanocrystals as fluorescent biological labels. *Science* **281**, 2013-2016, 1998.

[3] Gao X, Cui Y, Levenson RM, Chung LW, and Nie S. In vivo cancer targeting and imaging with semiconductor quantum dots. *Nat Biotechnol* **22**, 969-976, 2004.

[4] Park JW, Kirpotin DB, Hong K, Shalaby R, Shao Y, Nielsen UB, *et al.* Tumor targeting using anti-her2 immunoliposomes. *J Control Release* **74**, 95-113, 2001.

[5] Ballangrud AM, Yang WH, Palm S, Enmon R, Borchardt PE, Pellegrini VA, *et al.* Alpha-particle emitting atomic generator (Actinium-225)-labeled trastuzumab (herceptin) targeting of breast cancer spheroids: efficacy versus HER2/neu expression. *Clin Cancer Res* **10**, 4489-4497, 2004.

[6] Wiercioch R, Balcerczak E, Byszewska E, and Mirowski M. Uptake of radiolabelled herceptin by experimental mammary adenocarcinoma. *Nucl Med Rev Cent East Eur* **6**, 99-103, 2003.
[7] Kurebayashi J, Otsuki T, Tang CK, Kurosumi M, Yamamoto S, Tanaka K, *et al.* Isolation and characterization of a new human breast cancer cell line, KPL-4, expressing the Erb B family receptors and interleukin-6. *Br J Cancer* **79**, 707-717, 1999.
[8] Fujimoto-Ouchi K, Sekiguchi F, and Tanaka Y. Antitumor activity of combinations of anti-HER-2 antibody trastuzumab and oral fluoropyrimidines capecitabine/5'-dFUrd in human breast cancer models. *Cancer Chemother Pharmacol* **49**, 211-216, 2002.
[9] Ballou B, Lagerholm BC, Ernst LA, *et a*l. Noninvasive imaging of quantum dots in mice. *Bioconjug Chem* **15**, 79-86, 2004.
[10] Lovric J, Bazzi HS, Cuie Y, *et al.* Differences in subcellular distribution and toxicity of green and red emitting CdTe quantum dots. *Nano lett* **4**, 2163-2169, 2005.
[11] Hoshino A, Fujioka K, Oku T, *et al.* Quantum dots targeted to the assigned organelle in living cells. *Microbiol Immunol* **48**, 985-994, 2004.

NANO-SENSING CAPSULES FOR MEDICAL APPLICATION: NANO-PARTICLES FOR SENTINEL NAVIGATION AND QUANTUM DOTS CONJUGATION WITH ANTI-HER2 ANTIBODY FOR MOLECULAR IMAGING OF CANCER

NORIAKI OHUCHI, MORIO NAKAJIMA, HIROSHI TADA, TAKANORI ISHIDA

Department of Surgical Oncology, Graduate School of Medicine, Tohoku University 1-1, Seiryo-machi, Aoba-ku, Sendai 980-8574, Japan

MOTOHIRO TAKEDA

Department of Bioengineering and Robotics, Graduate School of Engineering, Tohoku University, Sendai, Japan

HIDEO HIGUCHI

Biomedical Engineering Research Organization, Tohoku University, Sendai, Japan

Nanomedicine is the application of nanotechnology to prevention, diagnosis and treatment of human disease. It has a potential to change medical science dramatically in the 21st century. However, the research field is in its infancy, and it is necessary to grasp mechanism of pharmacokinetics, the toxicity on the occasion of application to medical treatment, in particular on the aspect of safety of the materials and devices. Here, we describe fluorescent nono-particles for sentinel node navigation for breast cancer surgery in experimental model, which have shown the potential to be an alternative to existing tracers in the detection of the sentinel node of if we select the appropriate particle size and wavelength. We also describe generation of CdSe nanoparticles, Quantum Dots (QDs) conjugated with monoclonal anti-HER2 antibody, Trastuzumab, for molecular imaging of breast cancer cells. The QDs-Trastuzumab complex coated with PEG was successfully made without decreasing the titer of antibody. We established a high resolution of 3D *in vivo* microscopic system as a novel imaging method at molecular level. The cancer cells expressing HER2 protein were visualized by the nanoparticles in vivo at subcellular resolution, suggesting future utilization of the system in medical applications including drug delivery system to target the primary and metastatic tumors. Future innovation in cancer imaging, not only at cellular level but also at molecular level, by synthesizing diagnostic agents with nanoparticles, is now expected.

Keywords: Breast cancer, HER2 oncogene, Molecular imaging, Nanomedicine.

1. Introduction

Treatment for cancer with minimum invasive surgery without lymph nodes dissection based on sentinel lymph node (SN) navigation surgery has become a

major concern on the aspects of made-to-order and low-invasiveness medicine. Several radioisotopes and dyes are utilized for SN detection in standard methods, however, each detection method has advantages and disadvantages. To make up for the disadvantages, we aimed at developing a new non-invasive method using fluorescent beads of uniform nano-size that could efficiently visualize SN from outside the body and conducted experiments to determine the appropriate size and fluorescent wavelength. In this study, we examined the detection of SNs from outside the body using various particle sizes and wavelengths to determine the optimum size and wavelength, and confirmed that uniformly nano-sized fluorescent beads have the potential to be an alternative to existing tracers [1,2] in the detection of the SN in animal. These data should aid the adoption of a fluorescence measurement method in the future.

Anti-cancer therapeutics based on active tumor targeting by conjugating tumor-specific antibodies has become of great interest in oncology, pharmacology and nanomedicine. This approach will allow to increase therapeutic efficacy and to decrease systemic toxicity [3,4]. Quantitative investigation of dynamics of such delivery *in vivo* is crucial to enable the development of more effective drug delivery systems. One of best way to perform this is to apply new technology on biophysics field that the positions of proteins are detected quantitatively at single molecule level with nanometer precision [5]. However, the specific delivery processes *in vivo* is not known at single particle level. Conventional imaging modalities such as computed tomography, magnetic resonance imaging, positron emission tomography and organic fluorescence or luminescence imaging have insufficient resolution to analyze the pharmacokinetics of drugs at the single particle level *in vivo* [6].

To address the issue, real-time single particle tracking using quantum dots (Qdots) has been applied to the study of drug delivery. Qdots fluorescence nanocrystals, were thought to be as the marker because of their intense brightness and stability, in contrast to organic dyes and GFP [7,8]. In cultured cells, single particle tracking has yielded invaluable information on the function of purified proteins [9,10]. Recent work shows the antibody-conjugated Qdots have allowed real-time tracking of single receptor molecules on the surface of live cells [11]. However, no real-time single particle tracking in live animals have been reported, and it is uncertain that single particle of Qdots could be observed and tracked in live animals.

We analyzed the movement of single functional Qdots in tumors of mice from a capillary vessel to cancer cells. To observe single Qdot particles in tumor tissue, we used a dorsal skin fold chamber (DSFC) model [12]. The imaging system, consists of confocal scanner unit employing a Nipkow type disc and the

electron multiplying charge coupled device camera, facilitates high resolution *in vivo* single particle tracking at a video rate with spatial resolution of 30 nm. Quantitative and qualitative information such as velocity, directionality and transport mode was obtained using time-resolved trajectories of particles.

2. Materials and Methods

2.1. *Fluorescent beads as tracers for sentinel node navigation*

We used "FluoSpheres®" manufactured from high quality, ultraclean polystyrene microspheres (Molecular Probe Inc, OR. USA). We selected beads of sizes 20, 40, 100, and 200 nm and fluorescent colors of yellow-green (YG) (excitation/emission maxima at 505/515 nm), dark red (DR) (660/680 nm), far red (FR) (690/720 nm) and infrared (IR) (715/755 nm). The beads diameter distribution is very small, 0.02 ± 0.004μm in 20nm size and 0.1 ± 0.005μm in 100nm. We designed a laser scanning fluorescence detection system, which consists of three lasers, a resonant scanner (resonant frequency/200 Hz), a rotational pulse-stage and a CCD camera (Fig. 1). We used a diode pumped solid-state blue laser (473nm, 7mW) as the excitation source of YG fluorescent beads. For excitation of DR, FR, and IR fluorescent beads, we used a He-Ne laser (632.8 nm, 14.6 mW) or a laser diode (657 nm, 3.56 mW). The inguinal and femoral areas were continuously irradiated and scanned over an area of 30x50 mm. The fluorescence image was observed using a CCD camera (XC-EI50, Sony) with an optimum band-pass filter for each fluorescent bead.

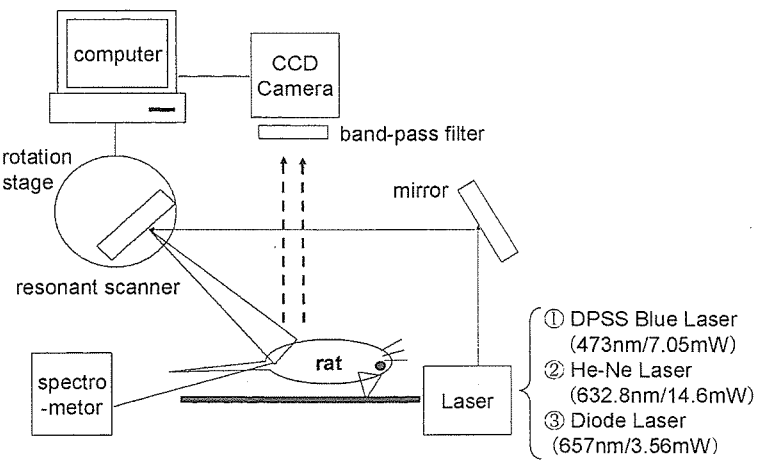

Fig. 1. Fluorescence imaging system for sentinel node detection using nano-sized particle.

In addition the spectrum of scanned area was analyzed with spectrometer. Under ether anesthesia, the hair of rats' lower body was removed to avoid autofluorescence of it. Then 50μl of FluoSpheres® 2% w/vol suspension was

subcutaneously injected at the footpad of the hind leg. Spectral analysis of fluorescence from rats injected with beads was performed to clarify the signal to noise ratio of fluorescence from beads and autofluorescence (Fig. 2). After observation from outside the body (through the skin) for 30-180 minutes, we peeled back the skin at the subcutaneous layer and ascertained the area of lymph nodes with navigation of their specific fluorescence. Then, the lymph nodes were removed, fixed with formalin and embedded in paraffin. Afterwards histological observation was performed with HE stain to confirm that the tissue was a lymph node.

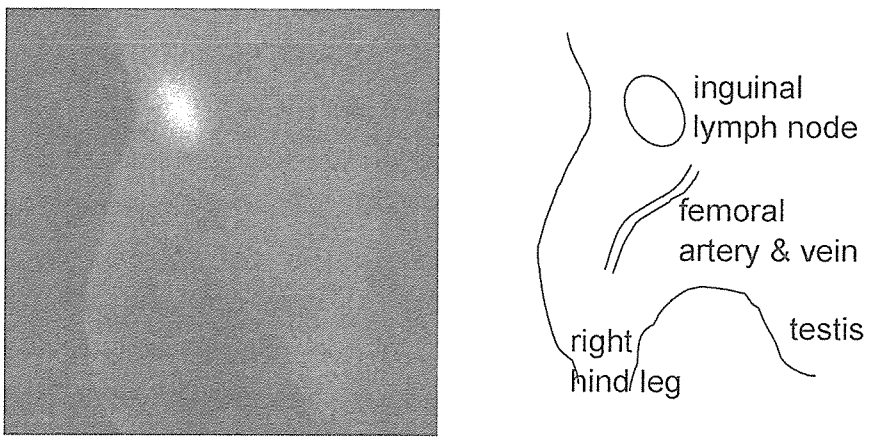

Fig. 2. Fluorescence image of right inguinal node and its illustration for sentinel node imaging using nano-sized fluorescent particle in rat.

2.2. *Nano-crystal semiconductor quantum dots conjugated with anti-HER2 antibody for molecular imaging of breast cancer*

Qdot was conjugated to trastuzumab (Chugai pharmaceutical Co., LTD., Tokyo, Japan) with a Qdot 800 Antibody Conjugation Kit (Quantum Dot Corporation, Hayward, CA) via poly ethylene glycol (MW. 2000) and SMCC-crosslinkers. The final concentration of QT-complexes was determined by measuring the conjugate absorbance at 550 nm and using an extinction coefficient of 1,700,000 $M^{-1}cm^{-1}$ at 550 nm.

The human breast cancer cell line KPL-4 [13], which overexpresses HER2 and is sensitive to trastuzumab, was a kind gift from Dr. J. Kurebayashi (Kawasaki Medical School, Kurashiki, Japan). KPL-4 cells were cultured in Dulbecco's modified Eagle's medium supplemented with 5% fetal bovine serum. A suspension of KPL-4 was transplanted subcutaneously to the dorsal skin of female Balb/c nu/nu mice at 6-10 weeks of age (Charles River Japan, Yokohama, Japan). Several weeks after tumor inoculation, mice bearing a tumor volume of 100-200 mm^3 were selected. All of the mice were maintained in our

pathogen-free institutional facilities. All operations on animals were in accordance with the institutional animal use and care regulations.

QT-complexes were injected into tail vein of mice. The mice were placed under anesthesia by the intraperitoneal injection of a ketamine and xylazine mixture at a dosage of 95 mg/kg and 5 mg/kg, respectively. The temperature of mice was maintained at 37 °C by a thermo-plate and objective lens heater. The modified DSFC method [12] was used to fix the exposed mouse tumor on the stage of the microscope. Two sterilized polyvinyl chloride plates (0.5mm thickness) containing a window were mounted so as to fix the extended double layer of dorsal skin including the tumor site. Skin between chambers sutured with 6-0 nylon around the window, and the tumor could be located in the center of the window and fixed without influence from the beating of the heart and/or breathing. The tumor was placed surface down on the neutral saline mounted cover slip on a viewing platform of an inverted microscope. The mouse was fixed to a metal plate on the stage designed to stabilize the chamber. Tumors can be visualized directly by means of this set-up.

The mice were sacrificed by CO_2 overdose, after imaging. The tumors were removed and divided for histological and immunohistochemical examination. In the histological Qdot uptake study, tumors were frozen and cryosectioned 6mm at thickness, fixed with acetone at 0°C and examined with an imaging system. For immunohistological examination, tumors were fixed in 10% neutral-buffered formalin overnight and then transferred into ethanol before processing and paraffin embedding. Immunohistochemical analysis was performed on paraffin sections at 6 mm thickness using the HercepTest (Dako Cytomation, CA).

As shown in Fig. 3, the optics system for 3D observation consisted primarily of an epi-fluorescent microscope (IX71, Olympus) with modifications, a Nipkow lens type confocal unit (CSU10, Yokokawa) and an electron multiplier type CCD camera (iXon 887, Andor). The confocal unit adopts multi-beam scanning using about a thousand beams that are simultaneously emitted through a pin-hole disk to facilitate high-speed scanning. And the EMCCD has advantage that offering unsurpassed sensitivity performance, and has been shown to yield markedly improved signal/noise ratio. The object lens was moved from a piezo actuator with a feedback loop for stabilizing the position of the focus. A computer controlled the piezo actuator in synchronization with the image acquisitions in order that the object lens remained within the exposure time of the CCD camera. An area of ~30 x 30 μm^2 was illuminated by a green laser (532 nm, Crystalaser).

The xy-position of the fluorescent spot was calculated by fitting to a 2D-Gaussian curve. The single molecule could be identified by the fluorescence

intensity. And quantitative and qualitative information such as velocity, directionality and transport mode was obtained using time-resolved trajectories of particles. The resolution of the position was determined from the position of immobile QT-complexes in a chemically fixed tumor cell. The resolution of the x and y directions of images taken at an exposure time of 33 ms was 30 nm taking into consideration the standard deviation.

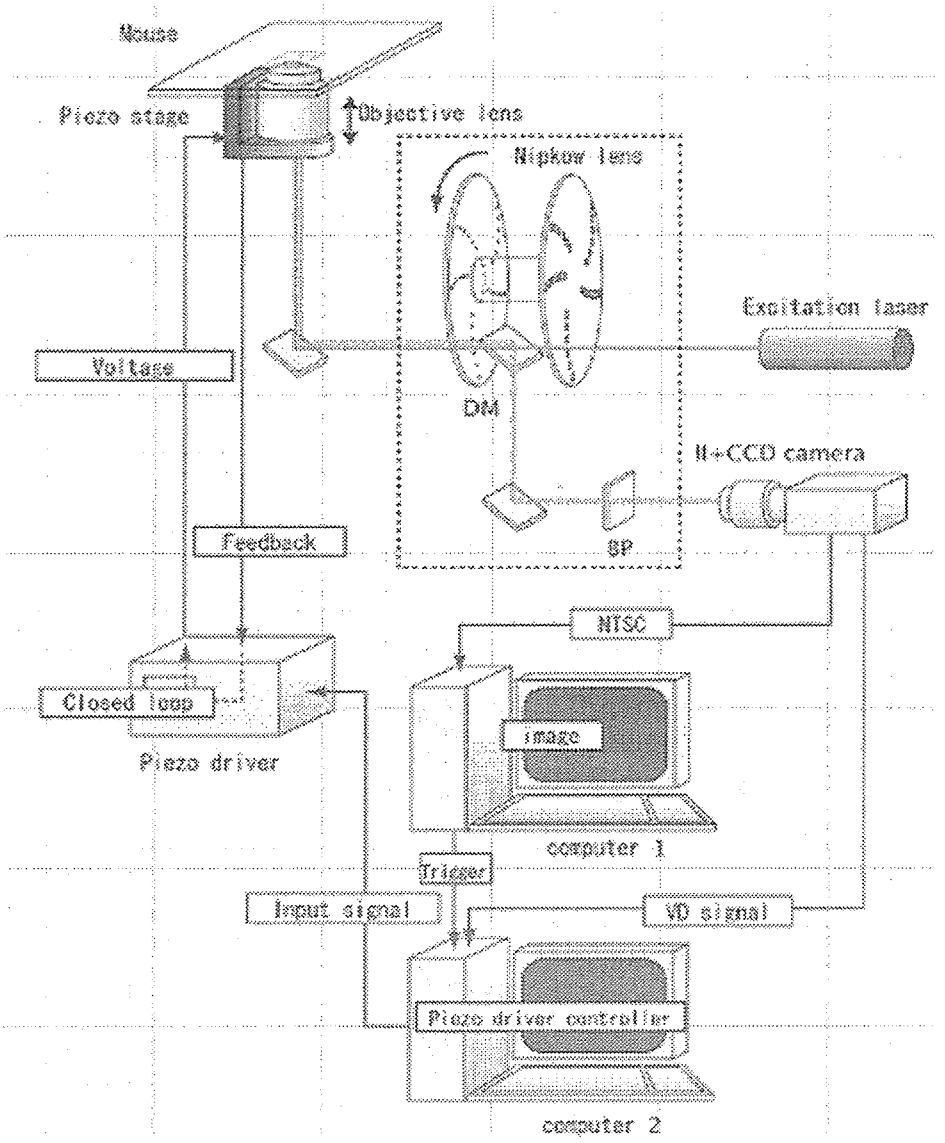

Fig. 3. The 3-D intravital imaging system for visualization of QT-complex in mice.

3. Results

3.1. *Fluorescent beads as tracers for sentinel node navigation*

We conducted the experiment on four types of beads with diameters of 20, 40, 100 and 200 nm. In the experiment using 20 nm beads, 22 feet from 13 rats

were tested. SNs were detected in 10 feet of 22 (45%) by fluorescence contrast. The time of detection from injection was 0 to 6 minutes. The average time for detection was 2.5 minutes and the median time was 2 minutes. With 40 nm beads, SNs were detected in 50 of 72 feet (69%). The time of detection from injection was 0 to 28 minutes. SNs in 42 feet were detected within 5 minutes. It was the most representative case (84%). The average time was 4.6 minutes and the median time was 3 minutes. With 100 nm beads, SNs were detected in 2 of 10 feet (20%). The average and median times were both 56 minutes. With 200 nm beads, SNs were detected in 7 of 18 feet (39%). The average time was 127 minutes. The median time was 135 minutes. In the 40 and 20 nm experiments, there was a significant difference in both the positive rate and average time. In the same way, we compared 40 with 100 or 200 nm beads severally.

We investigated three excitation and emission wavelengths with the 40 nm beads, Yellow-green (YG), Dark red (DR) and Infrared (IR). Beads of 40 nm in diameter were found to be the most suitable size in the previous experiment. In the experiment using YG, 10 feet from 5 rats were tested. SNs in 3 of 10 feet (30%) were observed by fluorescence measurement. With DR, SNs in 24 of 31 feet (77%) were observed and with IR, SNs in 23 feet of 31 feet (74%) were observed. DR and IR have advantage of positive rate of fluorescence detection as compared with YG.

Hemoglobin absorbs light in the range of visible light below 650 nm, and water absorbs light above 1100 nm. But in the near infrared range between 650 and 1100 nm, the absorption of light in living tissue is minimum. This range is called the optical window. Besides collagen, NADH and FAD are substances that *in vivo* have the fluorescent wavelengths in the range of 400 to 500 nm. So, from this point of view, NIR range has the advantage for the fluorescence measurement. In these experiments four different fluorescent wavelengths 515, 680, 720 and 755 nm were studied. DR and IR were more sensitive than YG in the detection rate experiments with 40 nm.

There was no significant difference in positive rate, but in average time between DR and IR. However, spectral analysis of DR and IR showed that IR has a higher signal-to-noise ratio compared than DR (Figs. 4a, 4b).

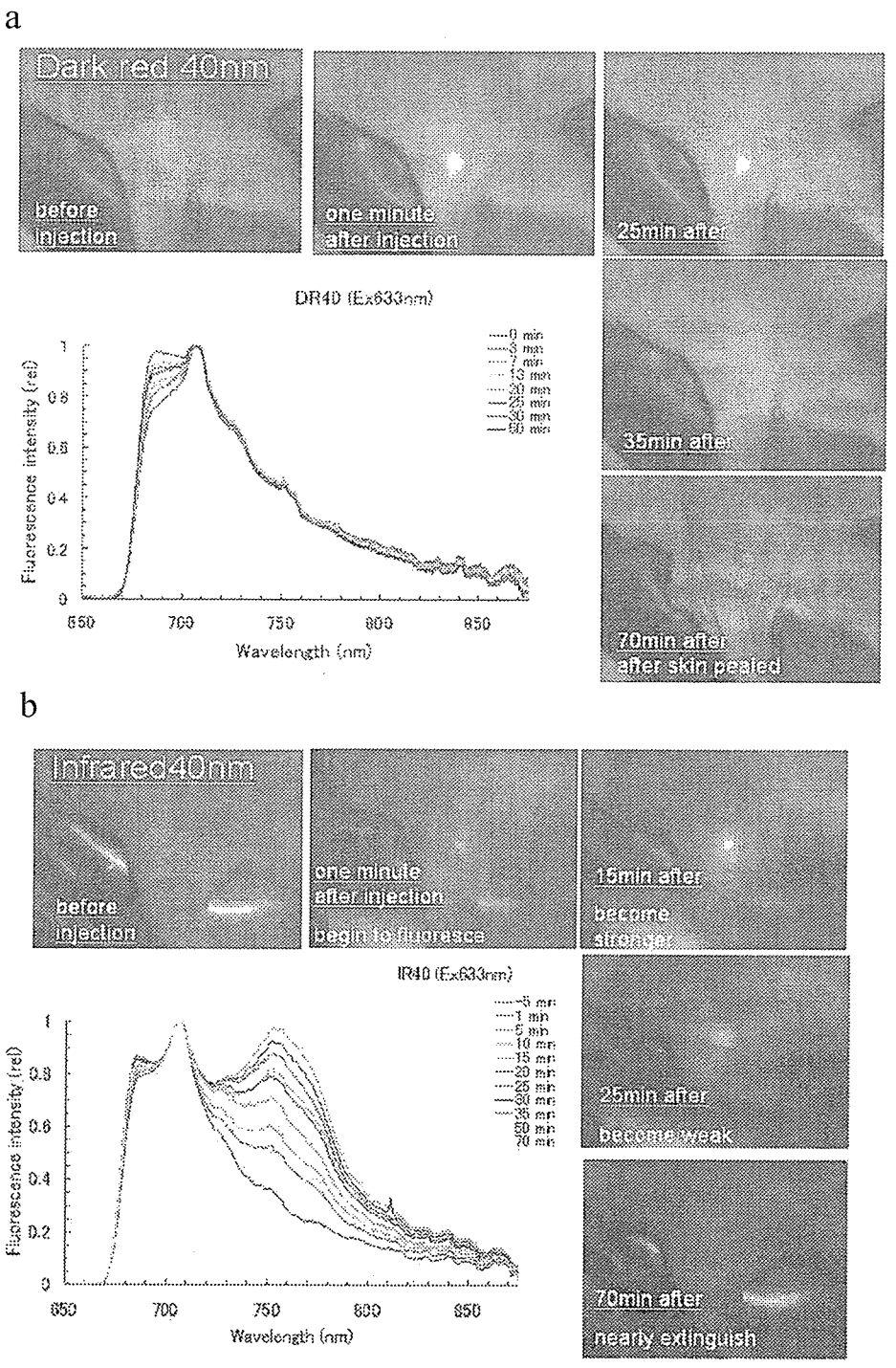

Fig. 4. Fluorescence image and spectrum analysis of right inguinal node after injection. a: Dark red-40nm-beads. The emission is strongest 30 minutes after injection. b: Infrared-40nm-beads. The emission is strongest 15 minutes after injection.

3.2. *Nano-crystal semiconductor quantum dots conjugated with anti-HER2 antibody for molecular imaging of breast cancer*

The conjugation of Qdots to trastuzumab using the Qdots antibody conjugation kit demonstrated that the molar ratio of trastuzumab to the Qdots was approximately 3:1. KPL-4, in which a human HER2 were overexpressed, was

cultured *in vitro*. KPL-4 cells were mixed with 10 nM QT-complexes for 5 minutes. QT complexes were bound strongly to the KPL-4 cell membranes. Six hours after the mixing, the signals from the QT-complexes were found mainly inside the cell near the nucleus, suggesting that the QT-complexes were endocytosed. Qdots without trastuzumab did not bind or accumulate in the KPL-4 cells. A control study using AH109A cells, a HER2 negative cell line, also showed no binding of the QT-complexes, indicating that QT-complexes selectively bind to the HER2 protein.

Tumor bearing mice model mice were prepared with KPL-4 subcutaneous implantation. Single Qdots in the tumor bearing mice were observed using a high resolution intravital imaging system through the DSFC. This system captures images of single Qdots at a video rate of 33 ms/frame. The DSFC was firmly mounted on the microscope stage to minimize the distorting influence of the heartbeat and breathing. 3D confocal intravital images of single QT-complexes were taken by moving an objective lens. 3D images of the tumor were taken by reconstructing 10 to 20-confocal images from the surface of the mice to a depth of 150 mm inside the tumor through the DSCF. Fluorescence micro-angiography was performed after injection of the QT-complexes into the tail vein. The membranes of the KPL-4 tumor cells were clearly stained with QT-complexes at 6 hours after the injection. At 24 hours after the injection, the QT-complexes had been internalized into the tumor cells (Fig. 5).

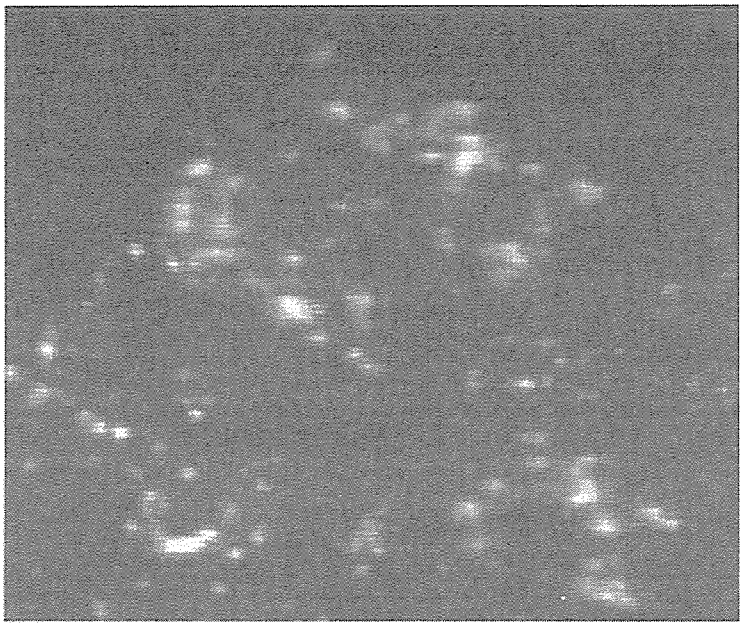

Fig. 5. 3D intravital imaging of KPL-4 breast cancer cells transplanted in living mouse. The QD-Trastuzumab complexes were observed not only at the cell membrane, but also in the cytoplasm of cancer cells.

After imaging the tumor in the living mice, histological examination of the chemically fixed tumors was performed to confirm that QT-complexes in the living mice exhibit activity on the KPL-4 cells. QT-complexes observed under the 3D microscope were located at the cell membrane and near the nuclear membrane. The position of the objective was fixed and 300-3000 sequential confocal 2D-images (total 10-100 seconds) were taken at this fixed position. Within 30 seconds after the injection, the current of the QT-complex in a vessel was observed. When a vessel and cells were clearly observable, the single QT-complex in the current in the tumor vessel was then analyzed. The fluorescence image of the circulating QT-complex was not a circle but an ellipse and sometimes a line at the video rate because QT-complex at times moved > 1mm in single frame. The speed of the movement of the single particles was calculated from the positional changes of the centroid of the QT-complex images. The average speed of each complex ranged from 100 to 600 mm/s, in agreement with a previous report by another method [14]. Each particle exhibited slow and fast movement in the blood stream. Such fast and slow movement characteristics could be induced by the pulse and nonuniform current within a vessel such as the Hagen-Poiseuille current. The slow speed of the complexes inside a tumor vessel would be important to locate pores between the vessel cells and then diffuse out from these pores.

Focusing on the vessel walls, a movement was observed of the complex extravasated from the intravascular space. The edge of the vascular inner-surface was not clear on a single frame image. Therefore, all the images obtained were averaged to precisely determine the position of the edge. The complexes were positioned first on the vascular surface and then extravasated. This is the first example of video rate observation of extravasation of very small particles, such as Quantum dots, in a mouse model.

Two hours after the injection, many complexes had migrated into the tumor interstitial area close to the tumor vessels. Most of the movement of the complexes was random in orientation and speed, indicating that complexes diffuse by the Brownian motion exerted by thermal energy. The average diffusion coefficient of the complexes was 0.0014 mm^2/s, much smaller than that at free diffusion in solution (~10 mm^2/s). Many complexes also moved randomly within a restricted small area of ~1 mm in diameter and then hopped by ~1 mm. The movement was restricted by a cage formed by the extracellular matrix.

Six hours after the injection, QT-complexes had bound to the KPL-4 cell membrane on which the HER2 protein is located. We successfully captured specific images of the QT-complexes bound to the cell membrane. Movements of single QT complex are identified in single frames. To identify the positions

of the tumor vessels and cells in living mice without further fluorescence staining, images were averaged. Many QT-complexes bound to the cell membrane exhibited Brownian motion within a restricted region of ~500 nm in diameter. The region is significantly larger than the area of ~30 nm which was drawn by position noise of the complexes fixed on a coverslip, indicating the movement is due to the anchor of the HER2 to a flexible component of the cytoskeleton such as an actin filament [15]. The QT-complexes restricted to the small area initiated linear movement in one direction along the cell membrane with speed of 400 to 600 nm and traveled for several micrometers.

We also observed in pursuing the transport of QT-complexes from the peripheral region of the cell to the perinuclear region. The QT-complex in a given cell moved almost straight toward the cell membrane with a velocity of 100-300 nm/s, changed direction to parallel to the cell membrane, and moved toward the cell nucleus at a velocity of ~600 nm/s. Finally, the directional movement of the QT complexes ceased and Brownian motion commenced within a small area, ~1 mm in a diameter, near the nucleus. The first two movements of straight towards and along the cell membrane would most likely be produced by the transport of an acto-myosin system binding to vesicle containing QT-complexes [16]. Because the actin filaments in cultured cells are highly concentrated in the peripheral region of cells. Movement toward the nucleus would most likely be on a microtubule transported by dynein [17] since there are almost no actin filaments near nucleus, but rather, a high concentration of microtubules.

4. Discussion

In the fluorescent nano-particle study for sentinel navigation surgery, homogeneous nano-sized beads have shown an advantage for efficient SN detection compared to existing colloids agents of heterogeneous size. Although the appropriate size for SN detection for human beings is predicted to be 500 nm and the optimum size may be different between animal species, the appropriate size should be determined for humans with accurately measured nano-sized beads of strictly same dimensions. There are two forms of transportation mechanism regarding a particle material to lymphatic system that is injected into tissue space. One is physical and active extracellular transportation; a particle passes through lymph capillaries. The other one is intracellular transportation of a particle. Foreign materials shift to the lymph capillaries after phagocytosis of particle. An investigation of *in vivo* dynamics of tracers is important in SN biopsy. It is reported that lymph node was detected by protected graft copolymer

combined with Cy5.5, or methoxypolyethyleneglycol-poly-L-lysine combined with Cy5.5 as a tracer. The nanoparticle may distribute to reticuloendothelial system as described in previous reports [18, 19], or may be excreted from kidney for their hydrophilia. We histologically observed liver and kidney two weeks after subcutaneous injection of fluorescent beads. Consequently, we didn't find beads trapped in liver or kidney by fluorescent microscopic observation, suggesting that the safety of these beads would be ensured when they are given *in vivo*.

The fluorescent beads that we used are mainly consisted of polystyrene. As polystyrene is the material often used for surgical strings in operation, there would be safe when we gave fluorescent beads to living organisms. Accumulation and toxicity are under investigation. The sample depth is a serious problem in fluorescence measurement of living tissue. The local excitation illumination within tissue exponentially attenuates due to absorption and scattering from the surface to that depth. This problem of lack of transmission prevents us from detection in tissues deeper than 1 cm from the surface of the body at present [10]. We can detect the SN of small animals like rats, but may have difficulty in detection in larger animals because of the depth at which SNs. For example, lymph node in human is buried in fat and it locates deeper than 1 cm. Detection technique to find SN up to 2 cm depth is recommended. Therefore, we are investigating the application of semiconductor nano crystal that has extremely stronger fluorescent intensity than usual fluorescent beads to increase the detection ability.

In the QD conjugation study for molecular imaging of cancer, we captured the specific delivery of single QT-complexes in tumor vessels to the perinuclear region of tumor cells in live mice after QT-complexes had been injected into the tail vein of mice. Six stages were detected (Fig. 6), 1) vessel circulation, 2) extravasation, 3) movement into the extracellular region, 4) binding to HER2 on the cell membrane, 5) movement from the cell membrane to the perinuclear region after endocytosis and 6) in the perinuclear region. The translational speed of QT-complexes in each process was highly variable, even in the vessel circulation. The movement of the complexes in each process was also found to be "stop-and-go", *i.e.*, the complex remaining within a highly restricted area and then moving suddenly. This indicates that the movement was promoted by a motive power and constrained by both the 3D-structure and protein-protein interactions. The motive power of the movements was produced by blood circulation (essential in processes 1 and 2), diffusion force driven by thermal energy (2, 3 and 4) and active transport by motor proteins (5). The cessation of movement is most likely induced by a structural barricade such as a matrix cage